Volume 24
Number 2

December *2022*
(ISSN 1109-1606)

Journal of

APPLIED ELECTROMAGNETISM

JAE

Institute of Communication and Computer Systems

Athens - GREECE

Volume 24 **December 2022**
Number 2 **(ISSN 1109-1606)**

JOURNAL
OF
APPLIED ELECTROMAGNETISM

Institute of Communication and Computer Systems

Athens - GREECE

Volume 24 **Number 2**

December 2022

TRANS BLACK SEA REGION UNION OF APPLIED ELECTROMAGNETISM (BSUAE)

JOURNAL OF APPLIED ELECTROMAGNETISM

Institute of Communication and Computer Systems

Athens - GREECE

Journal of Applied Electromagnetism

Copyright Form

The undersigned I confirm that I agree the publication of the article

in the Journal of Applied Electromagnetism and the copyright to belong to Trans Black Sea Union of Applied Electromagnetism. I understand that I have the full right to reuse this manuscript for my own purposes.

Name:

Surname:

Address:

E-mail:

Signed:

***Please send the previous form signed either by e-mail to pfrangos@central.ntua.gr , or by fax to the fax number: +30 210 772 2281, attention of Prof. P. Frangos.**

Address

Institute of Communication and Computer Systems,

National Technical University of Athens,

9, Iroon Polytechniou Str.,

157 73 Athens - GREECE

Tel: (+30) 210 772 3694

Fax: (+30) 210 772 2281, attention of Prof. P. Frangos

e-mail: pfrangos@central.ntua.gr

Web site: **http://jae.ece.ntua.gr**

TRANS BLACK SEA REGION UNION OF APPLIED ELECTROMAGNETISM (BSUAE)

JOURNAL OF APPLIED ELECTROMAGNETISM (JAE)

Volume 24 Number 2 December 2022

CONTENTS

HAND INFLUENCE ON THE MOBILE PHONE ANTENNAS' MATCHING TO THE FREE SPACE (selected from CEMA'22 Conference)

T. Nozadze , M. Kurtsikidze , V. Jeladze , G. Ghvedashvili 1

The goal of the research is to study the thermal effects caused by the electromagnetic (EM) field emitted by the mobile phone antenna. A novelty of the study is the hand Influence consideration on the mobile phone antennas' matching to the free space.

Inhomogeneous human model with different positions of the hand (fingers) and at different distances (1 mm, 10 mm, 20 mm) from the human head to the headset are studied;

The mobile phone antenna matching study to free space was carried out using the Finite-Difference Time-Domain (FDTD) method.

3700 [MHz] standard communication frequency was selected for numerical simulations.

NONLINEAR DYNAMICS METHOD IN THE APPLICATION TO THE STUDY OF TIME SERIES (selected from CEMA'22 Conference)

N. Ampilova 9

Time series are widely used for representation data of different types. Along the traditional methods the approach of nonlinear dynamics – reconstruction of the attractor of the system generating the series – is successfully applied. It allows us to calculate correlation dimension of the attractor of the system under study (if it exists) or to establish that the system does not have any attractor.

In this work we apply this method to solve a practical problem to analyze EEG records for revealing the patients with epileptic activity. Additionally, we calculate entropy of a signal on amplitude coverage. This approach resulted in separation of 15 records into 2 classes – epileptic activity and other pathologies, and it is in accordance with the expert conclusions.

The implemented program system may be used both for investigations and educational purpose, and the method may be applied to time series of other types.

APPLICATION OF MULTIFRACTAL METHODS FOR THE ANALYSIS OF CRYSTAL STRUCTURES (selected from CEMA'22 Conference)

I. Soloviev **19**

We discuss here images with complex structure such as biocrystals, which are very often turn out to be fractals or multifractals. We present 3 types of multifractal spectra, and vector characteristics based on using blanket technic for the surface of grey-level function constructed for a halftone or monochrome image. Such a set of characteristic describes the image structure quite complete. In this work we apply several different fractal and multifractal methods to analyse images. Our experiments make it obvious that for every class of images at least 2 methods allow obtaining reliable separation of numerical signs. The algorithms for calculation multifractal characteristics are implemented. For each class of images, the most appropriate signs were recommended.

HAND INFLUENCE ON THE MOBILE PHONE ANTENNAS' MATCHING TO THE FREE SPACE

(selected from CEMA'22 Conference)

Tamar Nozadze[*], Mtvarisa Kurtsikidze[**], Veriko Jeladze [***], Giorgi Ghvedashvili[****]

[*] Laboratory of Applied Electrodynamics and Radio Engineering, Ivane Javakhishvili Tbilisi State University, Tbilisi, Georgia

[**] Department of Engineering, Agrarian and Natural Sciences, Samtskhe-Javakheti State University, Akhaltsikhe, Georgia

[***]Department of Biocybernetics, Vladimir Chavchanidze Institute of Cybernetics of the Georgian Technical University, Tbilisi, Georgia

[****]Department of electric and electronic Engineering, Ivane Javakhishvili Tbilisi State University, Tbilisi, Georgia

E-mail: tamar.nozadze@tsu.ge

Abstract

The goal of the research is to study the thermal effects caused by the electromagnetic (EM) field emitted by the mobile phone antenna. A novelty of the study is the hand Influence consideration on the mobile phone antennas' matching to the free space.

Inhomogeneous human model with different positions of the hand (fingers) and at different distances (1 mm, 10 mm, 20 mm) from the human head to the headset are studied;

The mobile phone antenna matching study to free space was carried out using the Finite-Difference Time-Domain (FDTD) method.

3700 [MHz] standard communication frequency was selected for numerical simulations.

1. INTRODUCTION

Mobile phones have recently become an integral part of our lives. Naturally, interest arose in their impact on human health. Electromagnetic fields (EMF) emitted from mobile phone antennas interact with the human head and other parts of the body,

which in some cases can affect human health. Exposure to these electromagnetic fields is inversely proportional to the distance between the head and the mobile phone. But during communication, in most cases, the mobile phone antenna is in close proximity to the sensitive tissues of the human head. Therefore, the study of possible side effects associated with it is very relevant and important today.

As it is known, the energy absorption of EMF in tissues is characterized by the SAR coefficient (specific absorption coefficient [W / kg]), which is determined by the power absorbed by the unit of mass of the tissue. SAR is the only safety criterion for assessing the effects of this radiation on humans. Its thresholds are set by the Federal Communications Commission (FCC) in the USA and the International Commission on Non-Ionizing Radiation Protection (ICNIRP) in Europe [1]. Existing studies have shown that the interaction between an EM field and a biological object depends on the characteristics of the emitter [2]: its frequency, its location, and its orientation toward the object; On the shape of the emitted wave and the amplitude value of the EM field; As well as the ability of the biological body to absorb and accumulate energy [3].

Many publications show that absorption of radiated energy (SAR) depends on mobile phones and antenna types [4-5], its positions, and radiated power from the mobile phones [6]. The radiation nature and EM fields behavior depends on complex human body geometry [8], user's hand positions, other objects' existence around the user; where the user is located, in an enclosed or semi-enclosed space. But it's impossible to thoroughly quantitatively consider all these details.

Modern smartphones have AGC (Automatic Gain Control) and automatically increase the radiation power to establish a good connection in case the signal from the base station is weakened. The reactive field around the antenna increases. Because the reactive field area is larger than a cell phone with a hand, it covers all nearby objects with the ear, head, and hand. The result will be a large absorption at high reactive fields, which can be dangerous for humans' health [9].

The negative effects associated with these impacts are cumulative nature and may appear in the future. Of particular note are the harmful effects on children. They are exposed to RF radiation from an early age. The brain is the "main target organ" for this EM radiation. The nervous system of children and the brain are still unformed, the tissue

composition is relatively different (contains a relatively large amount of water, which has a permeability, the children's skull is much thinner, more permeable to this radiation than adults and therefore the negative impact in children can be more serious [8].

The goal of the proposed research is to investigate: how the hand and fingers different positions effects on the phone radiation parameter (S11 coefficient), which describes antenna matching to the free space;

2. METHODOLOGY

Since, the real experiments on human is not permitted, we will investigate scheduled tasks, by means of computer modelling. The Finite-Difference Time-Domain (FDTD) method [6], [9] will be used for numerical simulations. FDTD is the most suitable numerical method for computational analysis of complex-shaped and inhomogeneous objects like the human body. It gives us ability to use realistic nonhomogeneous human model in our research. However, the disadvantage of FDTD method is that we can't estimate the calculation error. Numerical experiments will be carried out using the EM and thermal solver of the proprietary FDTD based program package “FDTDLab”, developed at TSU (Laboratory of Applied Electrodynamics of the Tbilisi State University). The woman computer head model, named “Ella”, a 3D model with 1 mm discretization from "Virtual Population" (IT“IS Foundation) will be used for EM exposure simulations. Different hand configurations in holding the mobile phone (with different types of antennas) will be created by us (for example, phone held by fingers and phone held and covered by the palm) [9]. The considered head model consists of 47 types of tissues with different dielectric properties. For simplicity, the hand model will be filled with muscle material.

Frequency-dependent tissue parameters will be used from the known database (https://itis.swiss/virtualpopulation/tissueproperties/database/database-summary/).A sinusoidal waveform of 3700 MHz frequency will be used for simulations.

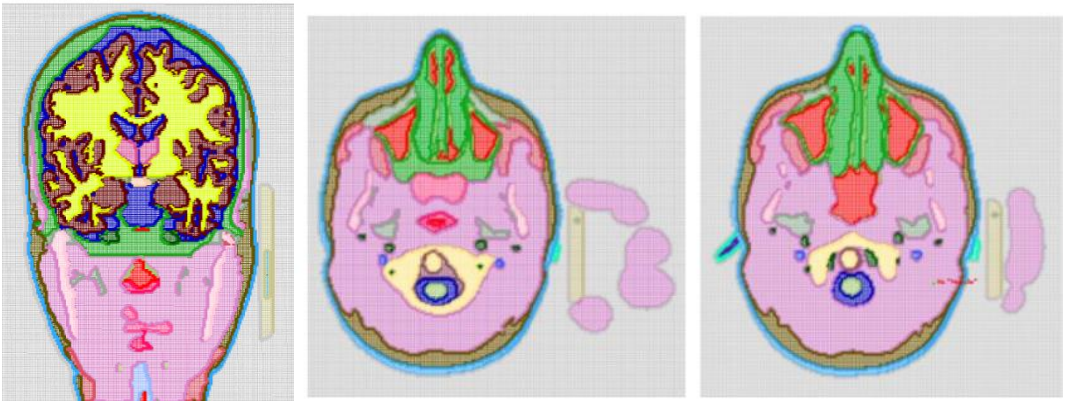

(a) (b) (c)

Figure 1. Woman discrete model: (a) without hand, (b) with hand 1, (c) with hand 2 at 3700MHz

For the human head model, two hand positions were prepared: When the mobile phone is held with fingers tip (hand 1), and when the mobile phone is held tightly with hand, touches the hand palm (hand 2) Fig. 1.

The mobile phone dimensions were (L × W × H) 5 × 0.8 × 9 [cm], with the dipole antenna embedded. The phone case permittivity was $\varepsilon = 2$.

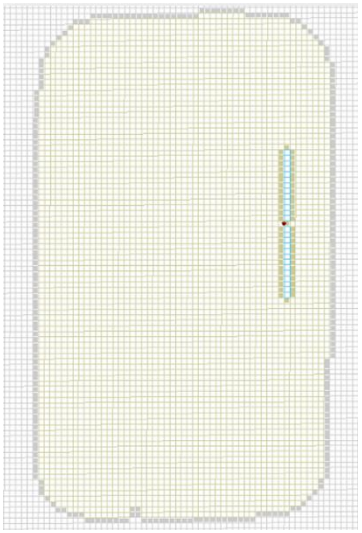

Figure 2. Mobile phone model with Dipole antenna.

The dipole length for the selected frequencies (3700 MHz) was selected so the S11 coefficient to be the lowest possible. In this case, the best antenna matching to open space was obtained. The length of the dipole antenna was 26 mm while the minimal S11 was 0.08 Fig. 2.

3. RESULTS OF NUMERICAL SIMULATIONS AND DISCUSSIONS

We studied frequency characteristics for a considered dipole antenna at the considered frequency, as it is shown on Fig. 3.

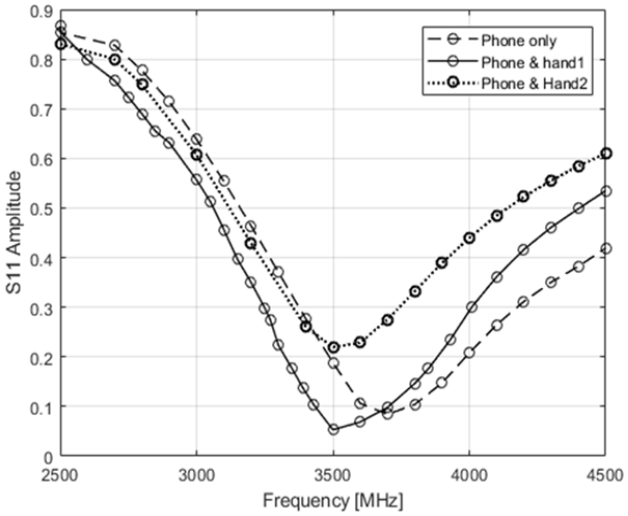

(a)

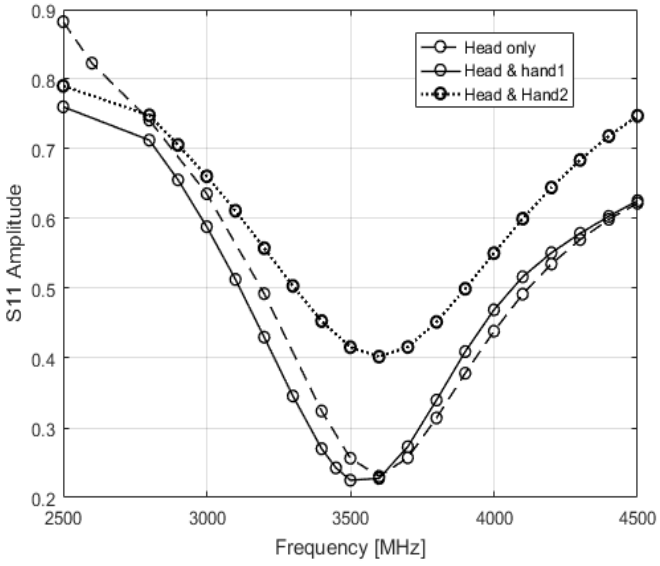

(b)

Figure 3. Dipole antenna frequency characteristics: (a) head without hand, (b) head with hand 1, and hand 2.

In both cases of numerical experiments hand considerations increase the S11 coefficient. In some cases, the head, hand, or fingers different positions reduce the S11 coefficient (this means that the antenna is well matched but at the shifted frequencies).

When mobile phone antenna is covered with a hand palm (hand 2) bad matching is observed (with and without head consideration) compared to the case when the mobile phone hold with a hand fingers (hand 1) Fig. 3.

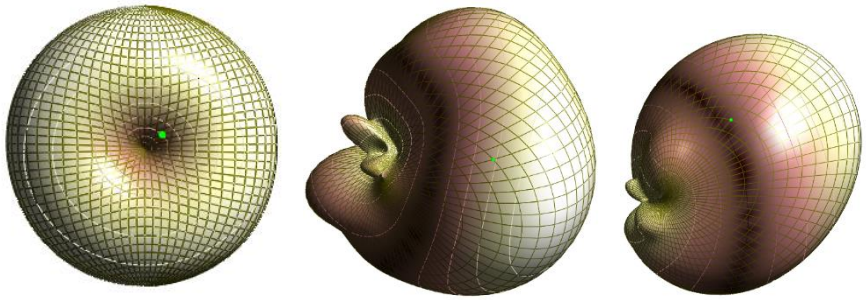

(a) (b) (c)

Figure 4. 3D radiation patterns for the mobile antenna without a head model at 3700 MHz: (a) only phone, (b) phone+hand 1, (c) phone+hand 2.

The 3D radiation patterns for the mobile antenna without a head and with different hand configurations are shown in Fig. 4, Fig. 5. It is well seen that the radiation patterns for the fixed-gain depended on the modelling scenarios.

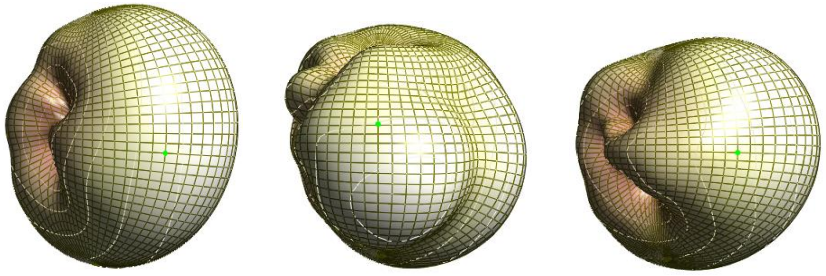

(a) (b) (c)

Figure 5. 3D radiation patterns for the mobile antenna with a head model at 3700 MHz: (a) phone+only head, (b) phone+head and hand 1, (c) phone+head and hand 2

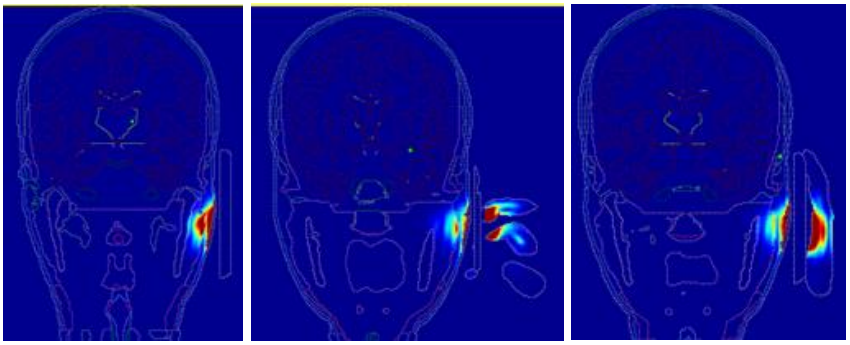

Figure 6. SAR distribution inside the human head-hand models at 3700 MHz: (a) head without a hand, (b) head and hand 1, (c) head and hand 2

Point SAR distribution inside the head-hand models is illustrated on Fig. 6. When the hand is considered, peak SAR locations were observed inside the hand. Because hand absorbs a big part of the EMF energy and therefore, SAR peak values in the head tissues are reduced.

4. CONCLUSION

In the present study, we investigated the impact of hand and head on mobile phone antenna matching conditions. The obtained results showed that hand consideration changes the antenna matching to the free space significantly.

The results of the research will be of great importance to each of us, and it will have a potential impact on the relevant industry and the wider community.

Research is not completed. The problems raised in the proposed paper are most significant and need further researches.

ACKNOWLEDGMENTS

Scientific research at the Ilmenau University of Technology (TU Ilmenau, Germany) was financially supported by the joint Rustaveli–DAAD fellowship programme 2022, ID 57646330, Grant number # 04/12, 25.05.2022.

Special thanks to Dr.-Ing. Prof. h. c. Karsten Henke (TU-Ilmenau, Germany) and Prof. Giorgi Ghvedashvili (TSU, Georgia).

REFERENCES

[1] ICNIRP, “Guidelines for limiting exposure to timevarying electric, magnetic and electromagnetic fields (up to 300 GHz),”.Health Physics, vol. 74, pp. 494-522, April 1998.

[2] J. Krogerus et al., "Effect of the human body on total radiated power and the 3-d radiation pattern of mobile handsets," IEEE Trans. Instrum. Meas., 56(6), p. 2375–2385, 2007.

[3] M. R. I. Faruque, et al., "Effect of human head shapes for mobile phone exposure on electromagnetic absorption," Informacije MIDEM-Journal of Microelectronics, Electronic Components and Materials, 40(3), pp. 232-237, 2010.

[4] M. R. I. Faruque et al., "Effects of Mobile Phone Radiation onto Human Head with Variation of Holding Cheek and Tilt Positions," Journal of Applied Research and Technology, vol. 12, pp. 871-876, October 2014.

[5] N. B. Rahman, et al., (2017) AzemiImpedance Analysis of Mobile Phone Antenna in the Presence of User's Hand. 2017 International Conference on Emerging Electronic Solutions for IoT (ICEESI 2017). https://doi.org/10.1051/matecconf/201714001031

[6] T. Nozadze, V. Jeladze, R. Zaridze, 'Mobile Antenna Matching Study Considering Different Holding Positions at 2100 MHz Frequency', XXVIth International Seminar/Workshop on Direct and Inverse Problems of Electromagnetic and Acoustic Wave Theory DIPED-2021, Tbilisi, Georgia, September 15-18, 2020

[7] V. Jeladze, M. Tsverava, T. Nozadze, V. Tabatadze, M. Prishvin and R. Zaridze,"EM exposure study on inhomogeneous human model considering different hand positions," XXI-th International Seminar/Workshop on Direct and Inverse Problems of Electromagnetic and Acoustic Wave Theory (DIPED 2016), Tbilisi, Georgia, September 26-29, 2016, pp. 9-12.

[8] J. Keshvari, M. Kivento, A. Christ and G Bit-Babik. "Large scale study on the variation of RF energy absorption in the head & brain regions of adults and children and evaluation of the SAM phantom conservativeness", Phys. Med. Biol. 61 (2016) 2991–3008.

[9] V. Jeladze, T. Nozadze, I. Petoev-Darsavelidze & B. Partsvania, "Mobile phone antenna-matching study with different finger positions on an inhomogeneous human model", Electromagnetic Biology and Medicine, Volume 38, 2019 - Issue 4. Published Online: 14 Jul 2019. https://doi.org/10.1080/15368378.2019.1641721

NONLINEAR DYNAMICS METHOD IN THE APPLICATION TO THE STUDY OF TIME SERIES (selected from CEMA'22 Conference)

N. Ampilova*

* St. Petersburg State University, Comp. Sci. Dept.

Email : n.ampilova@spbu.ru

Abstract

Time series are widely used for representation data of different types. Along the traditional methods the approach of nonlinear dynamics – reconstruction of the attractor of the system generating the series – is successfully applied. It allows us to calculate correlation dimension of the attractor of the system under study (if it exists) or to establish that the system does not have any attractor.

In this work we apply this method to solve a practical problem to analyze EEG records for revealing the patients with epileptic activity. Additionally, we calculate entropy of a signal on amplitude coverage. This approach resulted in separation of 15 records into 2 classes – epileptic activity and other pathologies, and it is in accordance with the expert conclusions.

The implemented program system may be used both for investigations and educational purpose, and the method may be applied to time series of other types.

1. INTRODUCTION

The notion of time series naturally appears in practice of data processing and statistical analysis. Time series is an ordered sequence of pairs of measured values, one if which is time and other may have a different nature and dimension. Time series are the results of experiments, both real and computational. In particular, the records of various signals are time series. Main problems for time series are Identification problem – for given observation data to find parameter of a system which generated this series.

Prognosis problem – for given observation data to predict future values of measured characteristics. The union of traditional methods of investigation of time series with the theory of dynamical systems lead to a new approach – the application of nonlinear dynamics methods to the investigation of time series of different nature, namely a reconstruction of the attractor of the system generating this series. [7]. The theoretical

substantiation of the reconstruction idea was given by F.Takens in [14]. It is based on the reconstruction of an attractor in a space of a suitable dimension where the attractor does not have self-intersection, i.e is embedded. According to Whitney's theorem if an attractor of a system lies in a n-dimensional space then it may be embedded in a space with dimension 2n+1. Namely this dimension (embedding dimension) is calculated by well-known Grossberg-Procaccia algorithm. This algorithm calculates the correlation dimension of the attractor, which is the same for the attractor in initial space and the space of embedding. The Grossberg-Procaccia algorithm is a time delay method [2], in which from a given scalar time series one form state vectors with a given time delay. Another method of this class is the method of false neighbors.

Seemingly, nonlinear dynamics methods for the first time were used in medical applications to analyze EEG records [1], [4], [12]. Later on they were applied in geophysics, astrophysics [3], physics, economics for the analysis of financial markets 15].

The application of reconstruction algorithms for EEG analysis meets many problems, the main of which is non-stationarity of a signal – the state of a patient during recording procedure may change. In this case the record should be divided on several periods in accordance with these states. Besides that, the record length may be insufficient for correct estimation of correlation dimension. The existence of stochastic noise is one more problem.

Research experience in this area shows that the choice of the parameters of reconstruction – time delay and the value of proximity (ε) between state vectors depends on the type of a record and its length. It was noticed in [8] that sometimes the length of time series does not allow the correct choice of ε, and a modified algorithm for the calculation of correlation dimension was proposed. In [9], [10] the author considered an optimized algorithm for calculation of correlation dimension.

Different algorithms and their implementations, and various variants of the choice of parameters naturally lead to different estimations for correlation dimension. However, researchers note that when solving many practical problems, it is the changing of correlation dimension (for different types of records) but not its value is important. In this situation an error in calculation is not essential, and the results of calculations retain their significance.

It was shown in [9] that correlation dimension EEG records for children 4-6 years (recorded in the state of rest) are essentially less than for adults. In [11] the author compared dimensions for 16 channels and revealed the synchronization of α-rythms in different parts of brain. The authors of [13] obtained the estimation of correlation dimension and separated EEG records of patients with two types of disease.

One of important characteristics of time series is entropy. It may be calculated on amplitude or time coverage. For this purpose, Shannon entropy and the class of Renyi entropies are widely used. In [3], [6] the authors applied so called permutation entropy to determine the degree of noise for a time series. The union of nonlinear dynamics methods and entropy characteristics gives a more detailed description of a system under study.

Thus, nonlinear dynamics methods are applied for solving the problems of time series analysis. In this work we present the program system for solving identification problem – reconstruction of the attractor of a system and estimation of correlation dimension of the attractor by a time series generated by the system, and calculation entropy characteristics. The paper has the following structure. In the next section main notions, the description of the methods of calculation of correlation dimension and the entropy for amplitude coverage are given. Section 3 contains the results of experiments for discrete and continuous dynamical systems and EEG records.

2. MAIN NOTIONS

Scalar time series is an array on N numbers which are values of a variable x(t) at the moments $t_i = t_0 + \tau(i-1)$,where τ is called sampling period [7]. We should make a remark about the choice of parameter τ.

Time series may be obtained as trajectories of discrete dynamical systems or results of numerical integration of continuous ones. In the first case $\boldsymbol{\tau}$ =1, at that time in the last case parameter $\boldsymbol{\tau}$ is the step of the numerical method. When recording signal from encephalograph, this parameter depends on the recording device. It means that the time between two consecutive values of time series depends on the method of its forming. As the result, when showing restored attractor, we may obtain different representations.

2.1. Takens method

Let $\varphi_t(x)$ be a n-th order dynamical system defined on a compact N-dimensional manifold M, and let we obtained a time series as a result of observation of the system functioning on a coordinate j. Then $\varphi_\tau^j(x)$ is the value of j-th component of $\varphi_t(x)$ at the time τ. If the system has an attractor $A \subset M \subset R^n$, it may be restored in Euclidean space with dimension $2N + 1$.

Define the map $F: M \to R^{2N+1}$ as the follows $F(x) = \left(\varphi_0^j(x), \varphi_\tau^j(x), \dots \varphi_{2N\tau}^j(x)\right)$, where τ is a period of the sample. In what follows we omit the denotation j for simplicity. Construct the vectors from the data of the time series $z_0 = (\varphi_0(x), \varphi_1(x),\dots,\varphi_{2N}), \dots z_i = (\varphi_i(x), \varphi_{i+1}(x),\dots,\varphi_{i+2N}), \dots, z_{K-2N} = (\varphi_{K-2N}(x), \varphi_{K-2N+1}(x),\dots,\varphi_K)$, where K is the length of the segment of the time series. In other words we construct z_i as a point in the space R^{2N+1}. By the Takens theorem [14] F is embedding M in R^{2N+1}, and it is the generic property. Hence, we have two systems: $\varphi: M \to M$, and $F: M \to R^{2N+1}$, which are connected by a nondegenerate change of variables $z = F(x)$. There is the characteristic that is invariant with respect to this change — correlation dimension, and we may obtain the properties of the attractor of the initial system as the properties of its copy in R^{2N+1}.

To determine the dimension of the embedding we follow the algorithm proposed by Grassberg and Procaccia [5]. It proposes to find such N for which there exists a functional dependence between values of the time series. If the system has an attractor then the points (trajectories) constructed by the time series are close. To estimate the closeness of points we use correlation integral and then calculate correlation dimension of the attractor.

The correlation integral estimates the number of pairs of points (constructed vectors z_i) which are ε-close:

$$C(\varepsilon) = \lim_{K\to\infty} \frac{1}{K^2} \sum_{n,n_1=1}^{K} \theta\left(\varepsilon - \rho\left(z_n, z_{n_1}\right)\right), \quad (1)$$

where K is the size the sample and θ is the Heaviside function. The correlation dimension of the attractor is defined as

$$D_c = \lim_{\varepsilon\to 0} \frac{\log C(\varepsilon)}{\log \varepsilon}, \quad (2)$$

and calculated approximately by the least square method as the angular coefficient of the line in coordinates $(\log \varepsilon, \log C(\varepsilon))$.

Thus, by changing the length of vectors z_i (denote it by k) we calculate D_c. This value may reach a stable value or not. In the first case we take the minimal value of k for the dimension of embedding, otherwise we believe that our series is a random noise, not a dynamical system.

The restored attractor is usually shown in projection to R^2 or R^3. For the plane one use coordinates (x(t), x(t+τ)), in R^3 – (x(t), x(t+τ), x(t+2τ)). In this work we use the projection on the plane.

2.2. Entropy on amplitude coverage

Consider the distribution of a signal by amplitude levels. Let x_{max}, x_{min} be maximal and minimal values of the signal respectively, and $\Delta = x_{max} - x_{min}$.. Divide Δ on N parts (levels) and define X_i as the number of $x(t)$ belonging to level i.

Define the normed distribution $\{p_i\}$ as $p_i = \frac{X_i}{\sum_i X_i}$ and calculate Shannon entropy $H(N) = -\sum_{i=1}^{N} p_i \ln p_i$.

3. NUMERICAL EXPERIMENTS

The most appropriate way to verify the Takens method is to use dynamical systems having attractors. The length of the obtained series may be taken arbitrary long. We consider examples for 3 types of data:

3.1. Henon map

The transformation is defined on R^2 and given by the formula

$$x_{n+1} = 1 - 1.4x_n^2 + y_n$$
$$y_{n+1} = 0.3x_n$$

It is well known that Henon map has attractor. The results of calculations: correlation dimension on x coordinate $D_c^x = 1.31$, correlation dimension on y coordinate $D_c^y = 1.25$.

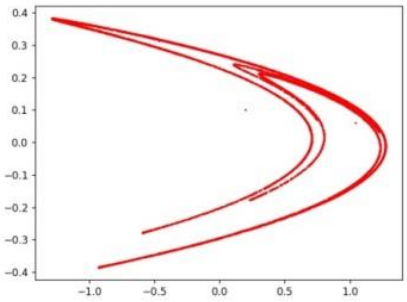

Figure1. Henon attractor. Initial point (0.2,0.1), 5000 iterations

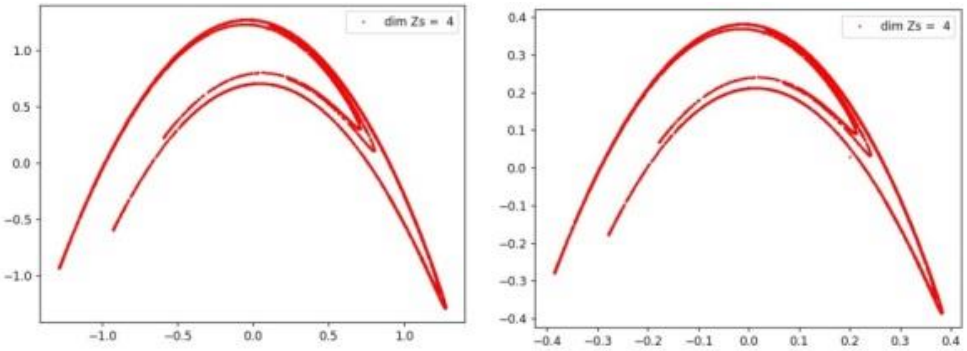

Figure 2. X- and Y- coordinate restored attractors for Henon map

3.2. Predator-prey system

The system is given by the system of differential equations and has the form

$$\dot{x} = (0.7 - 0.65y)x,$$

$$\dot{y} = (-0.35 + 2.7x)y.$$

For numerical integration we use 4th order Runge-Kutta method.

$$D_c^x = 1.05, D_c^y = 1.05.$$

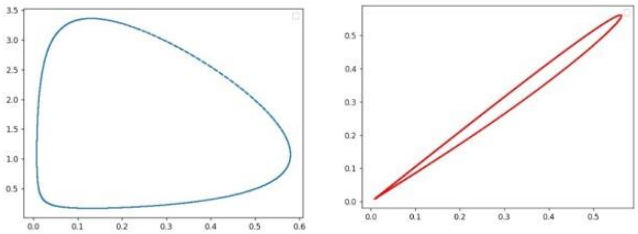

Figure 3. Attractor and x-coordinate restored attractor of predator-prey system. Initial point (0.5,0.55), 5000 iteration, $\tau = 0.1$

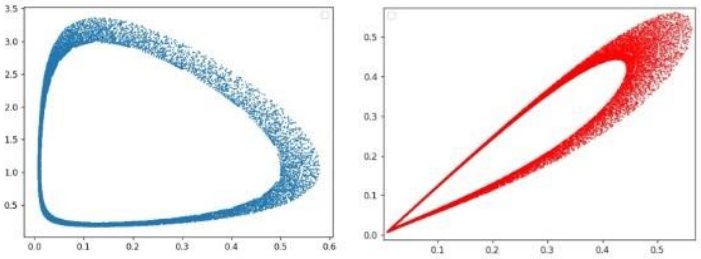

Figure 4. Attractor and x-coordinate restored attractor of predator-prey system Initial point (0.5,0.55), 5000 iteration, $\tau = 0.4$

3.3. EEG records

To calculate D_c we form vectors z_i by length k (starting from k=2) and calculate correlation integral for several values of ε by (2). Then we estimate D_c by the least square method. Increase k on 1 and repeat calculations. Compare obtained correlation dimensions. If they are close with a given accuracy δ we believe that the dimension reached a stable value. In this case we take the minimal value of k as the dimension of embedding. If dimensions are not close, we again increase k. In the situation when correlation dimension does not reach a limit value we consider the time series as a random noise, not a trace of a dynamical system.

It should be noted that one of main problems when calculating correlation integral is the choice of ε. Due to insufficient length of the time series it is difficult to take this parameter arbitrary, because the situation may occur when there are not pairs of points with such a distance between them. We use the following algorithm:

- take a sequence N_i of parts of a series by increasing length;
- for each N_i calculate distances between vectors z_i, z_j;
- take the minimal distance and one more as values of ε.

Note that to apply the least square method we need at least two values for ε.

We used 15 EEG records of patients with pathology and separated them into 2 classes – epileptic activity and other pathologies.

Example 1

Series length 514, frequency 80 Hz, time of recording 6.4s, the number of channels 16.

Results of calculation $D_c = 2.28, H = 1.37$ (using 0 channel)

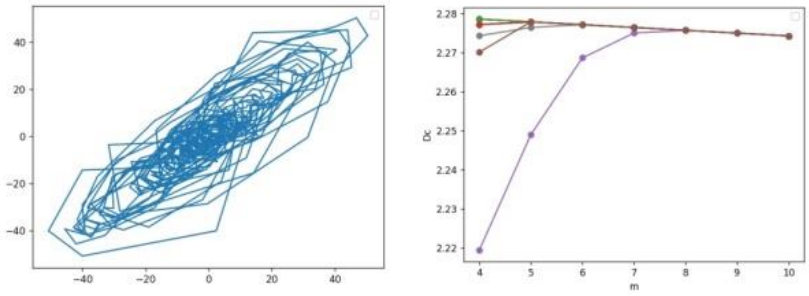

Figure 5. Restored attractor (0 channel) and the graph of stabilization of correlation dimension. Embedding dimension is 8

Example 2

The length of record 2139, frequency 80 Hz, time of recording: 26.73 s, 16 channels

$D_c \in [3.28\ ;\ 3.44]$, H=2.59 (using 0 channel)

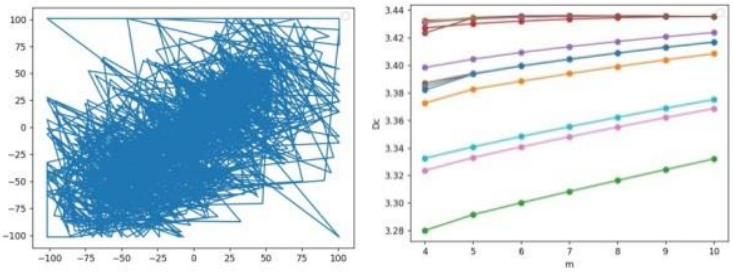

Figure 6. Restored attractor (0 channel) and graphs of correlation dimensions for 16 channels

Summarizing the results for 15 record one may conclude the following. 11 patients were preliminary considered by an expert as having epileptic activity, and 4 patients were diagnosed as having another pathology.

We use the value of interval were correlation dimensions and entropies on amplitude coverage lie. For records corresponding epileptic activity $D_c \in [2.27\ ;\ 2.46]$, and $H \in [0.99\ ;\ 1.37]$. In this case correlation dimension is practically the same for all channels, which means the synhronization process characterizing epilepsy.

For records of other pathology $D_c \in [0.6\ ;\ 1.5] \cup [3.10\ ;\ 3.44]$, $\mathrm{H} \in [2.02\ ;\ 2.59]$, and there is no synchronization. Thus, these signs allow the differing epileptic activity from other type of pathology.

6. CONCLUSION

In this work we implemented the investigation of time series by nonlinear dynamics method – reconstruction of attractor and estimation of correlation dimension. The entropy of a time series on amplitude coverage is calculated as an additional characteristic. Continuous and discrete dynamical systems having attractor and EEG records were considered as test examples.

For dynamical systems the correlation dimension is in accordance with known results, being the calculation is easier than for capacity dimension. For continuous systems the dependence of graphical representation of attractor on the choice of the step of numerical method is illustrated. For EEG records the implemented method allowed the separation of data on 2 classes, which in agreement with expert diagnosis.

These algorithms may be modified and applied to analysis of more complex time series.

ACKNOWLEDGEMENTS

The author thanks V. Lavruhin for help in computer experiments.

REFERENCES

[1] A. Babloyantz, A. Destexhe, "Low dimensional chaos in an instance of epilepsy". Proc. Nat. Acad. Sci. (USA), 1986, a3: 3513-3517.

[2] B.P. Bezruchko, D.A. Smirnov, "Mathematical modeling and chaotic time series", 2005 ,izd. GosUNZ "College", Saratov.(in Russian)

[3] O.V. Chumak, "Entropies and fractals in data analysis", https://www.researchgate.net/publication/235247584,2022-04-05 (in Russian)

[4] G.W. Frank, T. Lookman, M.A.H. Nerengerg, C. Essex, J. Lemieux, and W. Blume, "Chaotic time series analyses of epileptic seizures". Physica D, 1990, 46: 427-438.

[5] P. Grassberger, I. Procaccia "Measuring the strangeness of strange attractors.", Physica D. №1, v.9, 1983. P. 189-208.

[6] S.A. Makarkin, A.V. Starodubov, Y.A. Kalinin, "Application of permutation entropy in the analysis of chaotic, noise and chaotic-noise series", Journal of technical physics, 2017, v. 87, N. 11, .1712-1717.

[7] G.G. Malinezkii, A.B. Potapov, "Modern problems of nonlinear dynamics", 2002, URSS, Moskva (in Russian).

[8] O.Y. Mayiorov, V.N. Fenchenko, "Calculation of correlation dimension and entropy EEG signals on cluster computer systems", Klinicheskaia informatika I telemedicine,2014,v.10,N.11,10-20 (in Russian).

[9] A.A. Mekler, "Application of nonlinear analysis of dynamical systems for EEG signal processing", Vestnik novih medicinskih teknologii, 2007,v. Xiv, № 1, 73-77(in Russian).

[10] A.A. Mekler, "Program system for the EEG analysis by the dynamical chaos methods", PhD Thesis, SpB, 2006.(in Russian).

[11] D.A. Nikolaeva, "Application of correlation dimension method for analysis of EEG of patients with epilepsia",. Differential equations and control processes, №2, 2009,43-51,https://diffjournal.spbu.ru/pdf/darina.pdf (in Russian).

[12] J. Roschke, J. Aldenhoff, "The dimensionality of human's electroencephalogram during sleep", Biol.Cybernetics,1991,64,p 307-313.

[13] M.I. Shpitonkov, "Calculation of correlation dimension for physiological time series", Trudi ISA RAN,2020, v.702,75-79 (in Russian).

APPLICATION OF MULTIFRACTAL METHODS FOR THE ANALYSIS OF CRYSTAL STRUCTURES
(selected from CEMA'22 Conference)

I. Soloviev*,

* Saint-Petersburg State University

i.soloviev@spbu.ru

Abstract

We discuss here images with complex structure such as biocrystals, which are very often turn out to be fractals or multifractals. We present 3 types of multifractal spectra, and vector characteristics based on using blanket technic for the surface of grey-level function constructed for a halftone or monochrome image. Such a set of characteristic describes the image structure quite complete. In this work we apply several different fractal and multifractal methods to analyze images. Our experiments make it obvious that for every class of images at least 2 methods allow obtaining reliable separation of numerical signs. The algorithms for calculation multifractal characteristics are implemented. For each class of images the most appropriate signs were recommended.

1. INTRODUCTION

The study of the properties of various biological substances often uses the technique of obtaining their crystalline forms. In medicine, such methods of crystal growth as adding a substance to a solution of copper chloride, as well as adding a medicinal solution to an oil base, are well known.

In many cases, the properties of the substance under study can be judged by the type of crystal obtained. Methods of analysis and classification of digital images play an important role in the study of the properties of biocrystals. For example, in [1, 2] various approaches to the analysis of images of wheat samples are described, including using artificial neural networks.

Very often in applied problems of biology and medicine, researchers work in conditions of the so-called small sample, when the number of samples is in the tens, whereas most machine learning methods rely on the assumption of samples that differ by

orders of magnitude. Therefore, mathematical methods for obtaining fine classification features and the use of expert knowledge are of great importance here. Thus, in [3], the method of multifractal analysis was applied to the study of a set of 60 wheat samples. The obtained characteristics combined with expert assessments allowed us to divide the initial set into 5 classes.

The successful application of multifractal characteristics in the analysis of microscopic images of metal sections [4, 5] and in the study of nanostructures [6] shows that the same methods can be used in the analysis of such complex compounds as biocrystals.

The relevance of this research is due to an increasing number of areas in biological and medical research, where the results of experiments can be recorded by obtaining digital images using modern equipment.

In this work, we apply basic methods of fractal and multifractal analysis of digital images to the study of crystals of biological substrates and drugs, which is used in assessing the quality of biological products and laboratory control of drugs.

As classification features in this paper, we use the characteristics obtained by calculating such indicators as the Minkowski dimension, the Renyi spectrum and the multifractal spectrum determined by so called local density function, as well as parametrized spectra.

We show that decomposing an image into disjoint level sets using "local density function" allows filtering by selecting the set with the largest capacity dimension. Such sets preserve the main features of the original image, and the use of fractal technic allows for a clearer separation of images.

For images of various classes of biological substrates and drugs, we present the results of experiments.

ll papers must be written using Microsoft Word version 2 or newer. The fonts used must be Times New Roman, with size 14 for the Title of the paper, 12 for all the topics of the paper and 10 for the captions of figures and tables. Margins: Top and Bottom 2,54, Left and Right 3,17 in paper size A4.

2. MAIN DEFINITIONS

2.1. Fractal and multifractal characteristics

A natural characteristic of the sets of Euclidean geometry is their topological dimension. It is based on the concept of the multiplicity of the covering (the smallest number of adjacent elements of the covering, provided that the covering consists of elements having a finite size) and is an integer. Another approach to the notion of dimension was proposed by Hausdorff [7]. For a countable cover with a diameter of elements not exceeding a certain number, we consider a numerical series composed of the diameters of sets raised to a certain power p. The sum of the series is called the Hausdorff measure, it determines the value of at which the series converges. This value, which is not necessarily an integer, is called the Hausdorff dimension. It is known that for sets of Euclidean geometry, this characteristic coincides with the topological dimension. It turned out that the Hausdorff dimension can also be a characteristic for objects of a more complex structure, namely fractals. Such objects are characterized by fractional dimension. According to the definition proposed by the developer of fractal geometry B. Mandelbrot, a set is called fractal if its Hausdorff dimension is strictly greater than its topological dimension.

Fractal sets have the property of self-similarity. This means that the structure of a part of a fractal set is in some way "similar" to the structure of the whole set. Self-similarity can be strict and statistical. The sets for which the law of their construction is known (the Cantor set, the Serpinsky carpet, etc.) of course have strict self-similarity. Most natural objects with a complex structure can be considered as fractals (or multifractals) with statistical self-similarity.

Sets with strict self-similarity are usually constructed iteratively, from a formal point of view, the process of their construction is endless. When depicting such structures, it is believed that the constructed figure approximates the fractal well and gives a visual representation of its shape, if at a certain step of construction the differences become visually imperceptible.

2.2. Capacity dimension

In practice, calculating the Hausdorff dimension is a time-consuming task, therefore, the class of so-called "box-counting" (capacity) dimensions is used. The

method of calculation is to count the number of elements of linear size ε necessary to cover the set under consideration. When working with fractal sets, we assume that the so-called power law holds, namely, the number of elements of the cover $N(\varepsilon)$ is proportional to the linear size of an element in some degree,i.e. $N(\varepsilon) \approx c\varepsilon^{-D}$. This assumption is empirically conditioned.

Usually the capacity dimension of a nonempty bounded set $F \in R^n$ is defined as follows

$$D = \lim_{\varepsilon \to 0} \frac{\ln N(\varepsilon)}{-\ln \varepsilon}.$$

An approximate value of the capacity dimension can be obtained, for example, by using the least squares method.

2.3. Minkowski dimension

It should be noted that when analyzing images of fractal sets, the capacity dimension is determined only for black-and-white images.

To calculate the fractal dimension of the sets represented by halftone (gray-scale) images, we can use the Minkowski dimension. The method of calculation is based on the so-called blanket technic and does not use a coverage.

A detailed description of this method can be found in [7, 8], so we will provide here only the information necessary to describe the algorithm for its implementation.

Let $F = \{X_{ij}, i = 0,1, \dots, K, j = 0,1, \dots, L\}$ be a gray-scale image and X_{ij} be the gray level of the (i,j)-th pixel. This is a gray-level surface for the image, which can be viewed as a fractal for a certain measure range.

Let $F \subset \mathbb{R}^n$. Then δ-parallel body F_δ is a set of points being at a distance from F of no more than δ. i.e

$$F_\delta = \{x \in \mathbb{R}^n : |x - y| \leq \delta, y \in F\}.$$

We denote by $Vol(F_\delta)$ n-dimensional volume of F_δ. If for some constant s at $\delta \to 0$ the limit $Vol(F_\delta)/\delta^{n-D}$ is positive and bounded, then the number D is called the Minkowski dimension of the set F.

We build blankets u_δ, b_δ for a gray level surface as follows

$$u_\delta(i,j) = max\{u_{\delta-1}(i,j) + 1, max_{|(m,n)-(i,j)|\le 1} u_{\delta-1}(m,n)\}$$
$$b_\delta(i,j) = min\{b_{\delta-1}(i,j) - 1, min_{|(m,n)-(i,j)|\le 1} u_{\delta-1}(m,n)\}$$
$$u_0(i,j) = b_0(i,j) = X_{ij}$$

Point $F(x,y)$ is included in a δ-parallel body if $b_\delta(i,j) < F(x,y) < u_\delta(i,j)$. The definition of a blanket is based on the fact that the blanket for a surface of radius δ includes all the points of the blanket for a surface of radius $\delta - 1$ together with the points that are at the distance of 1 from this blanket.

The volume of a δ-parallel body is calculated by u_δ and b_δ:

$$Vol(F_{\delta)} = \sum_{i,j}(u_\delta(i,j) - b_\delta(i,j)).$$

The surface area is calculated using one of two formulas

$$A_\delta = \frac{Vol_\delta}{2\delta}$$

$$A_\delta = \frac{Vol_\delta - Vol_{\delta-1}}{2}.$$

Minkovsky dimension is defined as

$$D \approx 2 - {}^{ln\, A_\delta}/_{ln\, \delta}$$

To obtain the image characteristics, we use a vector $((\ln\delta, \ln A_\delta))$, the size of which is determined by the number of different values of δ.

2.4. Rényi spectra

Consider the set $M \subset R^n$, and its partition into $N(\varepsilon)$ cells with side (or volume) ε. We define the probability measure $p(\varepsilon) = \{p_i(\varepsilon)\}$, $i = 1, \dots, N(\varepsilon)$, $\sum_{i=1}^{N(\varepsilon)} p_i(\varepsilon) = 1$. Also consider the generalized statistical sum (or the sum of the moments of the measure) [9]

$$S(q,\varepsilon) = \sum_{i=1}^{N(\varepsilon)} p_i^q\,(\varepsilon), \qquad (1)$$

As usual we assume that the power law holds

$$p_i(\varepsilon) \sim \varepsilon^{\alpha_i}\ , \tag{2}$$

We also assume that the statistical sum itself also follows the power law:

$$S(q,\varepsilon) \sim \varepsilon^{\tau(q)}, \tag{3}$$

where $\tau(q)$ is a function of class C^1.

The symbol ~ in (2) and (3) is understood as follows:

$$\alpha_i = \lim_{\varepsilon \to 0} \frac{ln\ p_i(\varepsilon)}{ln\,\varepsilon},\ \tau(q) = \lim_{\varepsilon \to 0} \frac{ln\ S(q,\varepsilon)}{ln\,\varepsilon}, \tag{4}$$

Under these assumptions, the characteristic of a set with a complex structure is a set of generalized Renyi dimensions:

$$D_q = \lim_{\varepsilon \to 0} \frac{1}{q-1} \frac{ln\, S(q,\varepsilon)}{ln\,\varepsilon}, \tag{5}$$

2.5. Multifractal spectra

A multifractal set can be represented as a set of fractal subsets, each of which has its own fractal dimension. A multifractal spectrum is a set of dimensions of these subsets. Each subset is the union of covering elements having close values of exponents α_i in (4).

In this sense Renyi spectrum is not multifractal one, because it shows the changing of initial measure when parameter q changes. There is a connection between these spectra described by the Legendre transformation.

Namely, the transition from variables (q, $\tau(q)$) to variables ($\alpha, f(\alpha)$) may be done by the formulas

$$f\big(\alpha(q)\big) = q\alpha(q) - \tau(q), \tag{6}$$

$$\alpha(q) = \frac{d\tau(q)}{dq}. \tag{7}$$

and these relations are fulfilled on a special sequence of measures [10].

2.5.1 From Renyi spectra to multifractal ones through the Legendre transformation

Let M be a set and $\{M_i\}$ be its partition on $N(\varepsilon)$ cells by size ε. Consider a normed measure $\{p_i(\varepsilon)\}$ on $\{M_i\}$ and construct a sequence of measures $\mu(q,\varepsilon) = \{\mu_i(q,\varepsilon)\}$, where

$$\mu_i(q,\varepsilon) = \frac{p_i^q(\varepsilon)}{\sum_{i=1}^{N(\varepsilon)} p_i^q(\varepsilon)}, \tag{8}$$

Define the average $\alpha(q)$ of exponents α_i by a chosen measure

$$\alpha(q) = \lim_{\varepsilon\to 0} \frac{\sum_{i=1}^{N} \ln p_i(\varepsilon)\mu_i(q,\varepsilon)}{\ln \varepsilon}$$

For every measure $\mu(q,\varepsilon)$ calculate information dimension $f(q)$ of its support

$$f(q) = \lim_{\varepsilon\to 0} \frac{\sum_{i=1}^{N} \mu_i(q,\varepsilon) \ln \mu_i(q,\varepsilon)}{\ln \varepsilon}$$

It is not difficult to verify that these values are connected by the Legendre transformation, i.e formulas (6,7). In other words these relations are fulfilled on a special sequence of measures (8) (see [10]). The characteristics $\alpha(q), f(q)$ give a parametrized (by q) representation of multifractal spectrum and may referred to parametrized spectra. Excluding parameter q we obtain multifractal spectra $(\alpha, f(\alpha))$.

2.5.2. Immediate determination of multifractal spectra through local density function

This method was proposed in [11]. Consider an image I in R^2 and denote the square with center x and radius r (half of the side length) by $B(x,r)$. Denote the measure of pixel intensities by μ.

Assume that

$$\mu\big(B(x,r)\big) = kr^{d(x)}(x), \tag{9}$$

where $d(x)$ — local density function and k is a constant.

Consider (9) for r small enough, then it follows

$$d(x) = \lim_{r \to 0} \frac{\log \mu(B(x,r))}{\log r}$$

The function $d(x)$ characterizes the degree of heterogeneity of the pixel intensities distribution in a neighbour of *x*. The points *x* with local density *a* form the level set

$E_\alpha = \{x \in R^2 : d(x) = \alpha\}$. In practice we calculate α_{min}, α_{max}, $\alpha \in [\alpha_{min}, \alpha_{max}]$ and form the sets

$$E(\alpha, \varepsilon) = \{x \in R^2 : d(x) \in [\alpha, \alpha + \varepsilon)\}$$

where ε is a parameter.

We obtain a set of binary images. Obviously, this parameter controls the number of level sets and allows the separation of the image on nonintersecting level sets, and the procedure of separation is a kind of filtration.

Then we calculate capacity dimensions for level sets and obtain multifractal spectrum $f(\alpha)$.

3. NUMERICAL EXPERIMENTS

3.1. The effect of Cyna

The effect of Cyna 6 on biosubstrates was studied. The images from 2 classes (each contains 5 images) were analyzed by the methods described. The results are shown below.

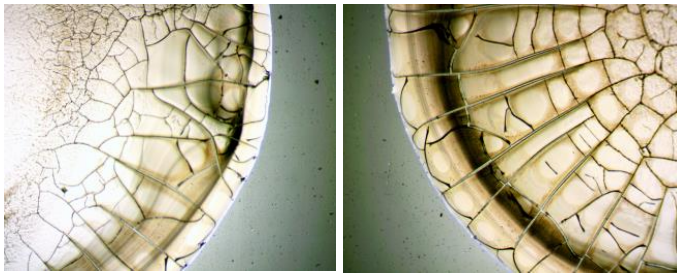

Figure 1. Biosubstrate without correction (left) and after correction (right)

Graphs are given below. All the calculated features show the separation.

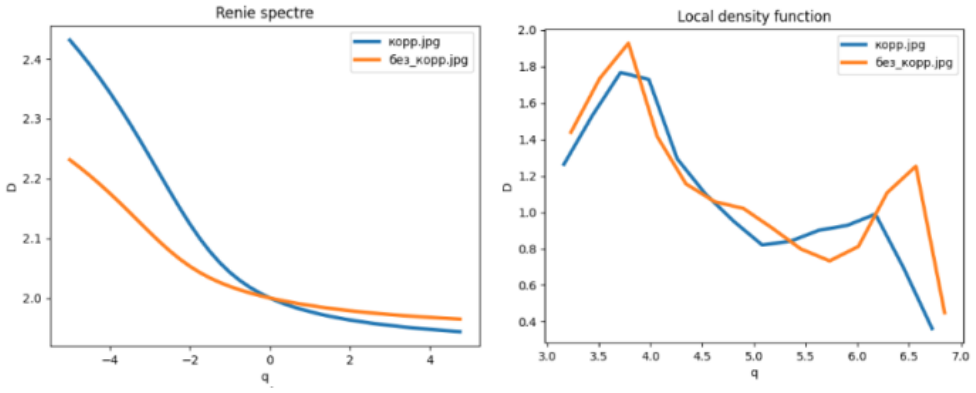

Figure 2. Renyi spectra and multifractal spectra by local density function

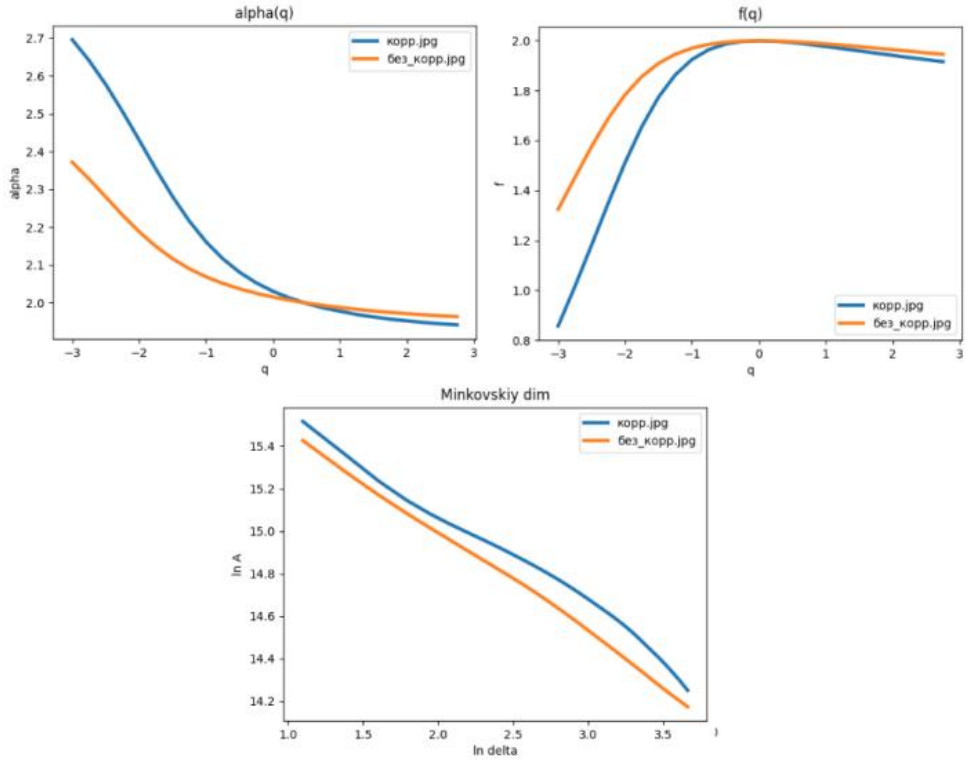

Figure 3. Parametrized spectra and graphs of characteristic vectors

3. 2 Crystals of drugs

Three types of crystals of drugs (medical solution is added to oil, crystals are formed on the boundary of matters). Images are obtained by microscope; every class contains 7-8 images.

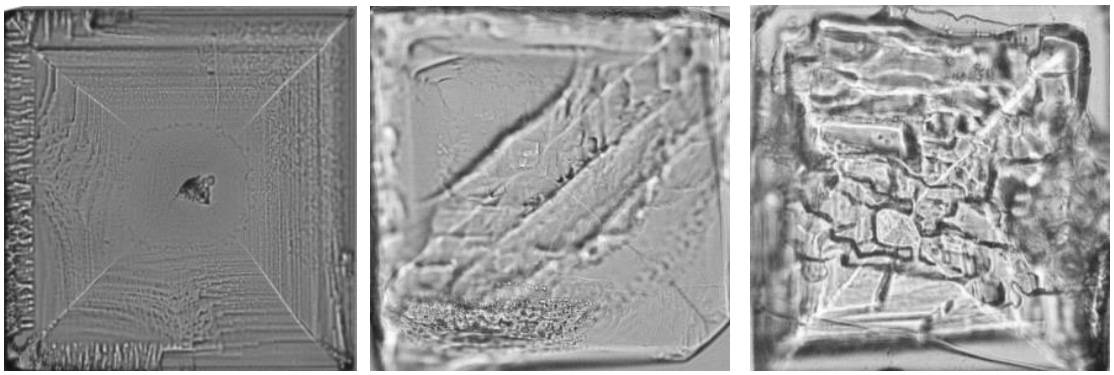

Figure 4. Class 1 (left), class 2(middle) and class 3 (right)

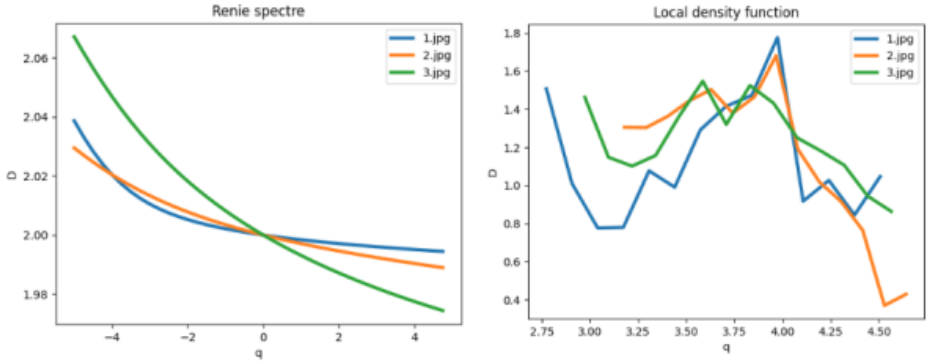

Figure 5. Renyi spectra and multifractal spectra by local density function

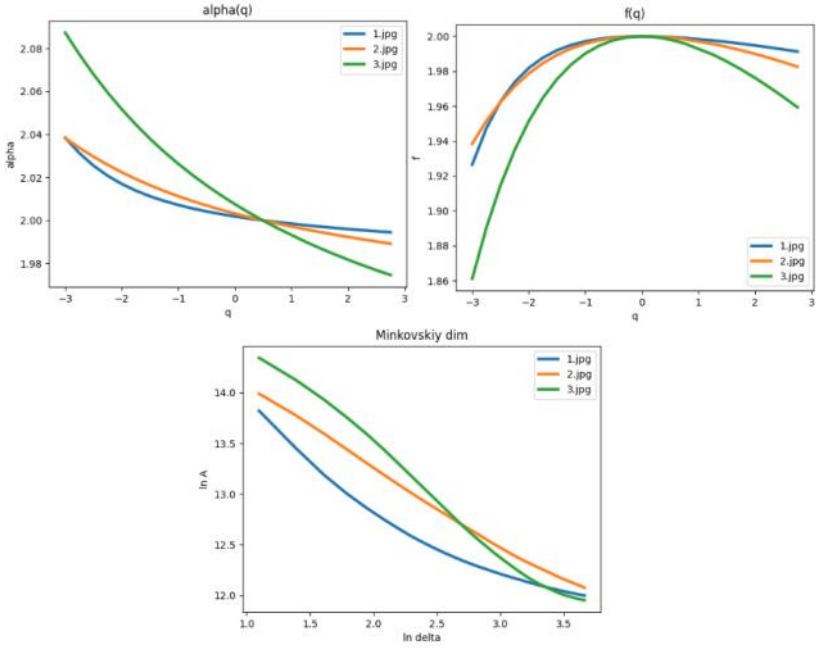

Figure 6. Parametrized spectra and graphs of characteristic vectors

5. CONCLUSION

As a rule, researches work with images biomedical preparations under conditions of so called small sample — the number of images is estimated in tens, not thousands. It is expert knowledge that has a decisive meaning. However, the practical experience shows that a description of images in terms of numerical characteristics is useful addition to visual perception. Any description of an image structure may be thought as a formalization of expert knowledge. In this work we demonstrate the results of application of several fractal and multifractal methods to analyze images of crystals of drugs. The experiments showed that for every class of images at least 2 methods allow obtaining reliable separation of numerical signs.

ACKNOWLEDGEMENTS

The author thanks I. Demidov for his significant help in organizing and performing the necessary numerical experiments.

REFERENCES

[1] A. Khoshroo, A. Arefi, " Classification of Wheat Cultivars Using Image Processing and Artificial Neural Networks", Agriculturial Communications, . — 2014, № 2 (1), p.17-22.

[2] P. Sadeghi-Tehran, " DeepCount: In-Field Automatic Quantification of Wheat Spikes Using Simple Linear Iterative Clustering and Deep Convolutional Neural Networks", Frontiers in Plant Science. 2019, v. 10. https://doi.org/10.3389/fpls.2019.01176.

[3] I. Murenin, N. Ampilova, "Analysis of Wheat Samples Using the Calculation of Multifractal Spectrum" , Computer Tools in Education, 2021, № 1,p. 5-20.

[4] G.V. Vstovsky, "Elements of information physics", M, MGIU 2002 (in Russian).

[5] A.Y. Bortnikov, N. N. Minakova, "Texturno-fractalnii analis microscopicheskih srezov obraztsov rompozisionnih materialov zapolnennih technicheskim uglerodom", Izv TPU, 2006. №6 (in Russian).

[6] S.V. Polischuk, K.A. Petrov, "Otsenka fraktalnyh svoystv nanostruktur po mikroskopicheskim izobrazheniyam", MNIG, 2022. №2-1 (116), in Russian.

[7] K. J. Falconer, "Fractal geometry", Chichester : Wiley,1990.

[8] Y. Y. Tang, C. Y. Suen, "Modified fractal signature (MFS): a new approach to document analysis for automatic knowledge acquisition", IEEE Transactions on Knowledge and Data Engineering,1997, 9, № 5,p. 747-762.

[9] S.P. Kuznetsov, "Dynamical chaos", M, Izd.fiz-mat lit.,2001 (in Russian).

[10] A. B. Chhabra, "Direct determination of the f(α) singularity spectrum and its application to fully developed turbulence" , Physical Review A.,1989,v. 40, № 9. p. 5284-5294.

[11] Y. Xu, H. Ji, C. Fermüller , Viewpoint Invariant Texture Description Using Fractal Analysis, International Journal of Computer Vision, 2009,v. 83, № 1,p. 85-100.